CONF-840387--13

DISCLAIMER

MULTIPHOTON IONIZATION OF ATOMIC CESIUM*

CONF-840387--13

DE85 001266

by

R. N. Compton, C. E. Klots, J.A.D. Stockdale, and C. D. Cooper**

Oak Ridge National Laboratory
Oak Ridge, Tennessee 37831

Presented at

Topical Meeting on Laser Techniques in Extreme Ultraviolet
Boulder, Colorado, March 5-7, 1984

*Research sponsored by the Office of Health and Environmental Research, U.S. Department of Energy under contract DE-AC05-84OR21400 with Martin Marietta Energy Systems, Inc.

**Department of Physics, University of Georgia, Athens, GA 30601.

MASTER

MULTIPHOTON IONIZATION OF ATOMIC CESIUM*

R. N. Compton, C. E. Klots, J.A.D. Stockdale, and C. D. Cooper**
Oak Ridge National Laboratory, Oak Ridge, Tennessee 37831

ABSTRACT

We describe experimental studies of resonantly enhanced multiphoton ionization (MPI) of cesium atoms in the presence and absence of an external electric field. In the zero-field studies, photoelectron angular distributions for one- and two-photon resonantly enhanced MPI are compared with the theory of Tang and Lambropoulos. Deviations of experiment from theory are attributed to hyperfine coupling effects in the resonant intermediate state. The agreement between theory and experiment is excellent. In the absence of an external electric field, signal due to two-photon resonant three-photon ionization of cesium via np states is undetectable. Application of an electric field mixes nearby nd and ns levels, thereby inducing excitation and subsequent ionization. Signal due to two-photon excitation of ns levels in field-free experiments is weak due to their small photoionization cross section. An electric field mixes nearby np levels which again allows detectable photoionization signal. For both ns and np states the "field induced" MPI signal increases as the square of the electric field for a given principal quantum number and increases rapidly with n for a given field strength.

Finally, we note that the classical two-photon field-ionization threshold is lower for the case in which the laser polarization and the electric field are parallel than it is when they are perpendicular.

INTRODUCTION

Multiphoton ionization (MPI) of alkali atoms has played a pivotal role in our understanding of the interaction of intense electromagnetic radiation with matter. The "hydrogen-like" energy levels and absence of low-lying autoionizing states make the alkali atom theoretically tractable. The low ionization potential and the ease with which one can produce atomic beams of alkali atoms facilitates the experimental studies. Many of the early MPI studies involved high-powered fixed-frequency lasers. Presently, the availability of tunable dye lasers with wavelength extension (i.e., frequency doubling, Raman shifting, etc.) makes it possible to study one- to six-photon ionization of the alkali atom with continuously tunable radiation. Also, harmonic generation in these systems which may be present during ionization can be recorded more easily than in other systems since the radiation generated is in the visible or

* Research sponsored by the Office of Health and Environmental Research, U.S. Department of Energy, under contract DE-AC05-84OR21400 with Martin Marietta Energy Systems, Inc.

** Department of Physics, University of Georgia, Athens, GA 30601.

near ultraviolet spectral region. The ability to tune the laser to high Rydberg states using either even or odd numbers of photons accesses electronic states of both parities. Stepwise excitation is capable of selectively producing states of high orbital angular momentum.

The angular distributions of photoejected electrons provide valuable information about the structure of atoms and molecules and the photoionization process itself. The photoelectron angular distributions depend upon the nature of the initial bound state and final continuum states. The continuum contribution involves the interference between the partial waves of the outgoing electron, and any interaction between this electron and the ion core. The electron angular distribution resulting from the electric-dipole interaction between a single photon and an isotropic distribution of atoms is given by

$$\frac{d\sigma(\lambda,\theta)}{d\Omega} = \frac{\sigma_{TOT}(\lambda)}{4\pi}\left[1 + \beta P_2(\cos\theta)\right] \tag{1}$$

where σ_{TOT} is the generalized photoionization cross section for one-photon ionization at wavelength λ, $P_2(\cos\theta)$ is the second Legendre polynomial, θ is the angle between the polarization axis of the incident light and the direction of the photoelectron K and the value of β is the so-called asymmetry parameter. β can vary continuously from -1 to +2.

In MPI, the order of the process (i.e., number of photons involved) and the possible participation of real and virtual intermediate states are the two most important factors which determine the angular distribution. For the case of nonresonant MPI or for resonantly enhanced MPI and when the laser intensity is weak enough to validate the lowest order perturbation theory, the generalized cross section for N-photon ionization can be written as

$$\frac{d\sigma(\lambda,\theta)}{d\Omega} = \frac{\sigma_{TOT}(\lambda)}{4\pi} \sum_{i=0}^{N} \beta_{2i} P_{2i}(\cos\theta) \tag{2}$$

where $P_{2i}(\cos\theta)$ is the 2ith order Legendre polynominal of order 2i and β_{2i} are functions of microscopic atomic parameters.

A number of theoretical studies of angular distributions of photoelectrons from MPI have been published.[1-5] Experimental measurements of angular distributions have been presented for two-photon ionization of sodium,[6,7] of titanium,[8] of cesium,[9] of strontium,[10] and five-photon (nonresonant) ionization of sodium.[11] The influence of nuclear spin on angular distributions has been studied for the case of sodium.[12] In addition, the effects of "quantum beats" due to the hyperfine levels on angular distributions have been observed.[13] Finally, angular distributions for so-called above threshold ionization of xenon at a fixed wavelength (0.53 μm) have been reported.[14] Both the experimental and theoretical studies have illustrated that measurements of angular distributions of photoelectrons from resonant MPI are complicated by the following:

1. The angular distributions may be laser power dependent due to saturation of some resonant level or due to a.c. Stark effects on the ground and excited states involved.[4,15]
2. So-called above threshold ionization[14,16] effects in which photoejected electrons gain energy from the radiation field may complicate the measurements.
3. If more than one hyperfine level is excited (which is most often the case), "quantum beat" interference effects produce angular distributions which are dependent upon the temporal characteristics of the laser beam. For example, in two-photon ionization, the photoelectron angular distribution for the two-photon ionization of sodium via the $3^2P_{3/2}$ state is found to depend upon the time delay between the exciting and ionizing laser pulses.[13]
4. Sometimes subtle background or surface ionization effects are observed which can interfere with (or even obscure) the real signal (see, e.g., Ref. 7).

The studies of photoabsorption in DC-electric fields is a well developed subject. First-order Stark shifts in hydrogen and second-order Stark shifts in other atoms have been exhaustively studied for the case of one-photon absorption. In this work we present the first experimental studies of the DC Stark effect upon MPI. As we shall see, the DC Stark effect can greatly enhance the MPI cross section both in the resonant excitation step and in the ionization step.

Experiments in which highly excited states are produced in external electric or magnetic fields allow one to test fundamental ideas about the electron-Coulomb system in the quasi-continuum.[17] In this work we describe studies of MPI in the presence of an electric field (E = 5 to 4000 V/cm) in which the plane of polarization of the laser can be rotated relative to the direction of the electric field. As we shall see, the Stark effect mixes nearby states of different parity, allowing for the detection of dipole forbidden states. Finally, we will show that the classical (two-photon) field ionization threshold is lower for the case when the laser polarization and the electric field are parallel than it is when they are perpendicular.

EXPERIMENTAL

The MPI photoelectron angular distributions were measured in an apparatus consisting of a collimated cesium beam which is directed into the entrance of a double focusing spherical sector electron energy analyzer. A laser beam is focused to a spot ~1 cm from the entrance hole. The acceptance angle is $\sim\pm2°$. The laser power density is $\sim10^8$ W/cm^2. Experiments involving the DC Stark effect on MPI were performed in a parallel field geometry. The laser beam was focused between two parallel plates separated by ~0.6 cm. The electric field could be varied from 0 to ~3 KV/cm. Ions were pushed through a grid in the negative plate and detected with a dual channel plate charged particle detector after drifting through a short time-of-flight mass spectrometer (~10 cm).

In both experiments, a Molectron model UV-24 nitrogen laser (~1 MW peak power) was used to pump the oscillator and amplifier of a Molectron model DL-14 dye laser. The bandwidth of the laser was ~0.2 Å (FWHM). A Glan-Air prism (Carl Lambrecht) was used to purify the laser beam and the polarization was rotated through a full 2π angle with one of two different Fresnel rhomb polarization rotators.

In both experiments the laser ionization signal is processed with a Princeton Applied Research boxcar integrator model 165. Figure 1 shows a typical recorder trace of the electron energy spectrum for three of the resonant intermediate states reported herein. The absolute energy scale was not established. Excellent self-consistency among all of the peaks was observed. That is, by establishing an energy scale for one resonant intermediate level such as for the $7p^2P_{3/2}$ state (as was done in Fig. 1), all other peaks would correspond to the expected values [i.e., $2h\nu$-IP (Cs) or $3h\nu$-IP (Cs)]. The best resolution obtained in any of the alkali studies was 0.07 eV with 0.1 to 0.2 eV resolution commonly used.

RESULTS AND DISCUSSION

A. Angular Distributions

Figure 2 shows the MPI photoelectron angular distribution for the case of two-photon ionization in which the first photon is in resonance with the $7p^2P_{1/2}$ state of cesium. Since no orientation of the $7p^2P_{1/2}$ state is expected from the transition $6s^2S_{1/2}$–$^27P_{1/2}$ the angular distribution will resemble a one-photon distribution, i.e., $I(\theta) = 1 + \beta_2 \cos^2\theta$ The experimental data shown in Fig. 2 are not corrected for the finite angular resolution of the electron spectrometer ($\Delta\theta = \pm 2°$). The finite angular resolution was mathematically unfolded from all of the experimental data in this work and the points in the unfolded distribution were almost indistinguishable from the original distribution. The difference in the two distributions was well within the uncertainty in the measurements. Kaminski, Kessler, and Kollath[18] have published angular distributions for the same transition and these data are in good agreement with the data shown in Fig. 2. Tang and Lambropoulos[19] have calculated angular distributions for the $7p^2P_{1/2}$ state according to the method of Dixit and Lambropoulos[20] and their calculations are shown as a solid line in Fig. 2. There is excellent agreement between experiment and theory.

The angular distribution for photoionization of the $7p^2P_{3/2}$ state is shown in Fig. 3. In this case the agreement between theory and experiment is poor. Although the general features of the experimental data are predicted, the theory is always well below the experimental points when normalized at $\theta = 0$ and π. The previous data of Kaminski, Kessler, and Kollath[18] in Fig. 4 shows even larger discrepancies. The rather large differences between the theory and the two conflicting experimental studies are believed to be due to the mixing of hyperfine levels in the $7p^2P_{3/2}$ state. The splitting between the two extreme hyperfine levels of the $7p^2P_{3/2}$ state is 198 MHz which corresponds to a hyperfine period of 5 ns. Our laser has

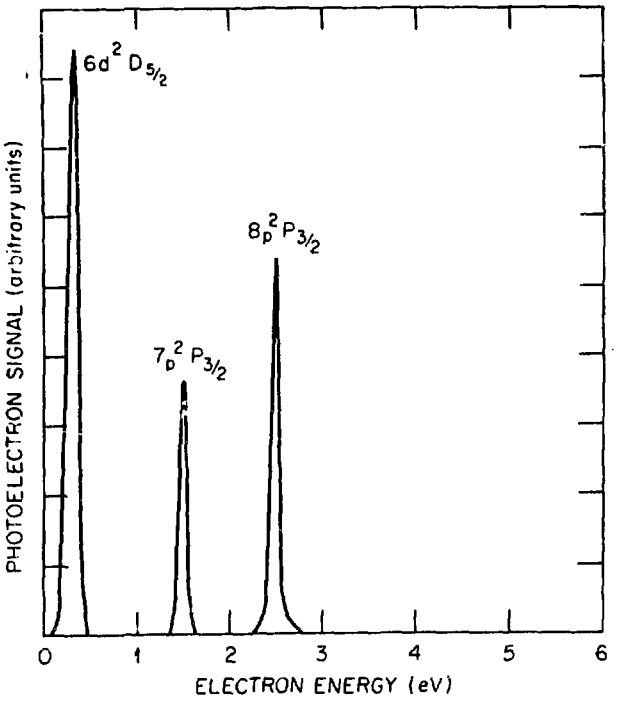

Fig. 1. Recorder traces of electron energy distributions for photoelectron produced by MPI of cesium. The energy scale was calibrated by fixing the $7p^2P3/2$ peak at its calculated energy position. The laser was tuned to one- or two-photon resonance with the states shown.

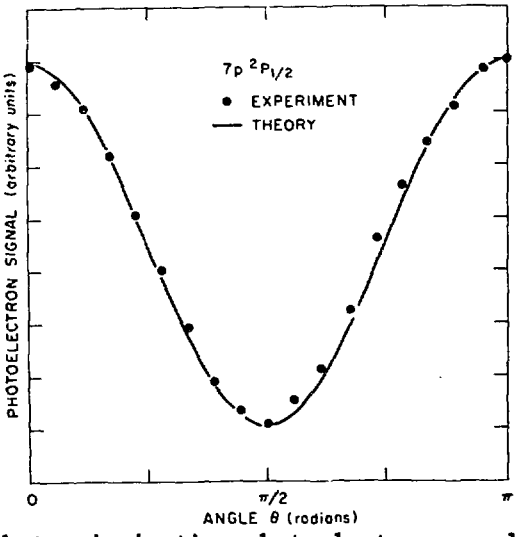

Fig. 2. Two-photon ionization photoelectron angular distributions in which the first photon is in resonance with the $7p^2P_{1/2}$ state. The theory is that of I. Tang and P. Lambropoulos.[19] The error bars in both intensity and angles are roughly twice the size of a data point.

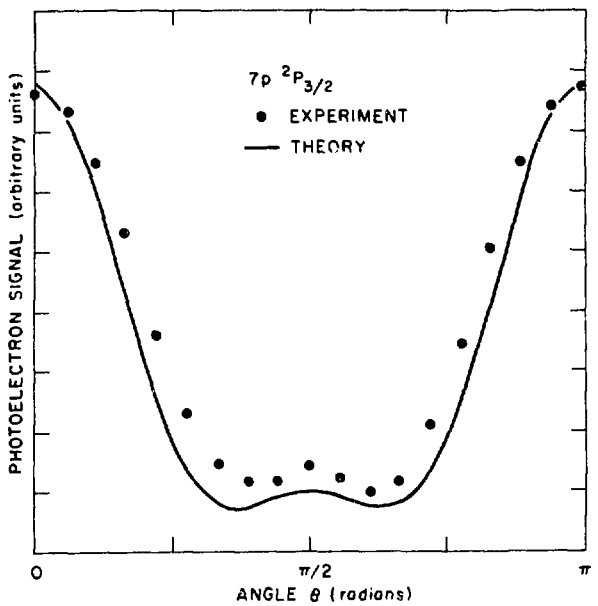

Fig. 3. Same as Fig. 2 except $7p1/2 \rightarrow 7p^2P3/2$ is also added. The slight difference in the two distributions is attributed to partical hyperfine mixing of the intermedite $7p^2P3/2$ level during the ~10 μs laser pulse. Theory is due to Tang and Lambropoulos.[19]

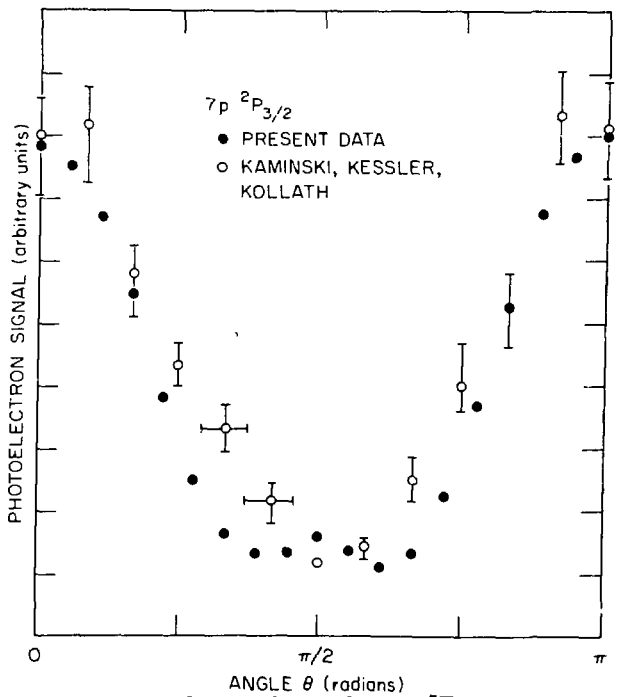

Fig. 4. Comparison of previous data [Kaminski, Kessler, and Kollath (KKK)][9] with the present data for the $7p^2P3/2$ state. The laser pulse width for the data of KKK is ~400 ns. The difference two sets of experimental in the data is attributed to complete hyperfine mixing during the laser pulse in the case of KKK. Theory is due to Tang and Lambropoulos.[19]

a pulse duration of ~10 ns which would allow for some hyperfine mixing during the excitation-ionization event. The flashlamp pumped laser of Kaminski, Kessler, and Kollath[18] had a pulse length of 400 ns allowing for complete mixing of the hyperfine levels thus producing the distribution shown in Fig. 3. The hyperfine period for the $8p^2P_{3/2}$ state is about twice as long as that for the $7p^2P_{3/2}$ and therefore we should expect better agreement between experiment and theory. Figures 5 and 6 show the experimental and theoretical results for the $8p^2P_{1/2}$ and $8p^2P_{3/2}$ states, respectively. The results further illustrate the effect of hyperfine coupling, i.e., the agreement for the $8p^2P_{1/2}$ state where no orientation occurs is excellent, whereas the theory for the $8p^2P_{3/2}$ again falls below the data.

Figure 7 shows the experimental angular distribution for the case of two-photon resonant three-photon ionization of cesium via the $8d^2D_{5/2}$ intermediate state. Here the hyperfine period is ~55 ns and the agreement between theory and experiment is good. In this case the laser pulse is over before hyperfine coupling can occur.

Tang and Lambropoulos[19] have developed a theoretical expression which takes into account the hyperfine effects on the angular distributions for the $7p^2P_{3/2}$ and $8p^2P_{3/2}$ resonant intermediate state. The theory satisfactorily accounts for the distributions presented in Figs. 3 and 4 and the data of Ref. 9.

B. Field Effects on Multiphoton Ionization

In these experiments an effusive atomic beam is crossed at right angles by tunable light from a nitrogen laser-pumped dye laser. Perpendicular to both beams, a variable, uniform electric field draws any resulting positive ions through a time-of-flight mass spectrometer into a channelplate charged particle detector. The angle Θ between the applied electric field $\vec{F}$ and the electric vector $\vec{E}$ of the laser beam is also continuously variable using a double Fresnel rhomb rotator.

As Fig. 8 illustrates, the MPI signal at low electric fields is greatly enhanced when the second photon is resonant with a nd level. The MPI signal is seen to drop rapidly with increasing principal quantum number ($\sim 1/n^8$), mainly due to the fact that the photoabsorption ($\sim 1/n^3$) and photoionization ($\sim 1/n^5$) cross sections are decreasing rapidly with n. The signal reappears as an approximate "step function" where a third photon is no longer necessary to effect ionization. As illustrated, this step occurs below the zero-field two-photon ionization potential. The shift Δ from the true IP, as a function of the electric field, F follows closely the familiar relation for field ionization:

$$\Delta = a|\vec{F}|^{1/2} \qquad (3)$$

with Δ and $|\vec{F}|$ in atomic units, and $\vec{E}$ parallel to $\vec{F}$ we find $a_{\parallel} = 1.90\ (\pm 0.03)$, close to the semi-classical value of 2. Upon rotating $\vec{E}$ perpendicular to F, the ionization threshold shifts to lower energy, consistent with the classical model of Cook and Gallagher.[21]

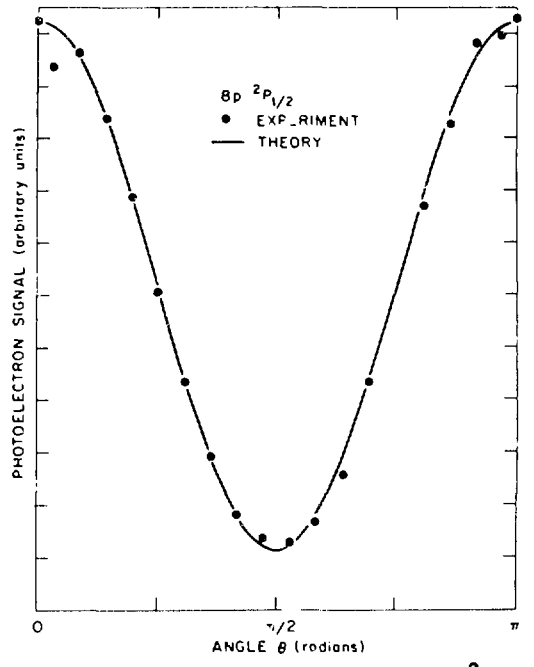

Fig. 5. Same as Fig. 2 except with the $8p^2P_{1/2}$ state.

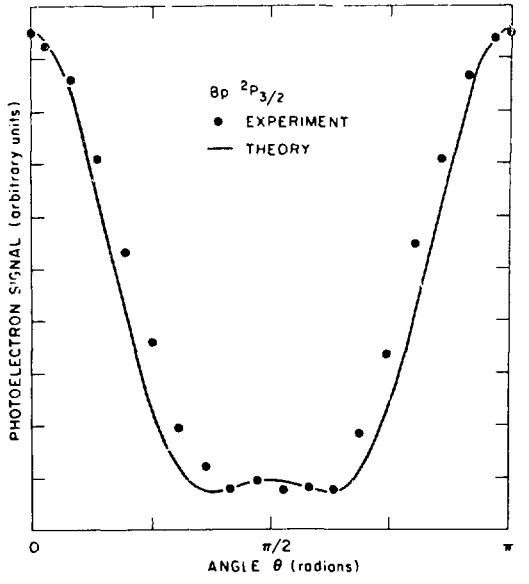

Fig. 6. Same as Fig. 3 except with $8p_{1/2} \rightarrow 8p^2P_{3/2}$.

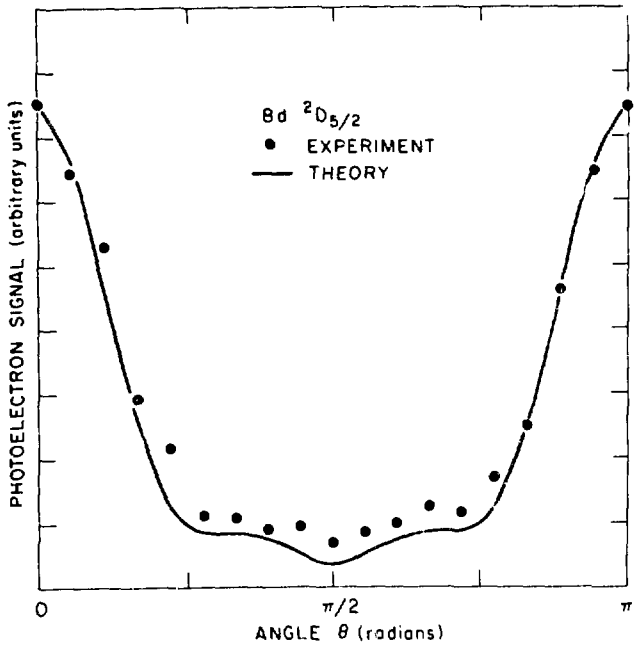

Fig. 7. Same as Fig. 2 except with the $8d^2D_{5/2}$ state.

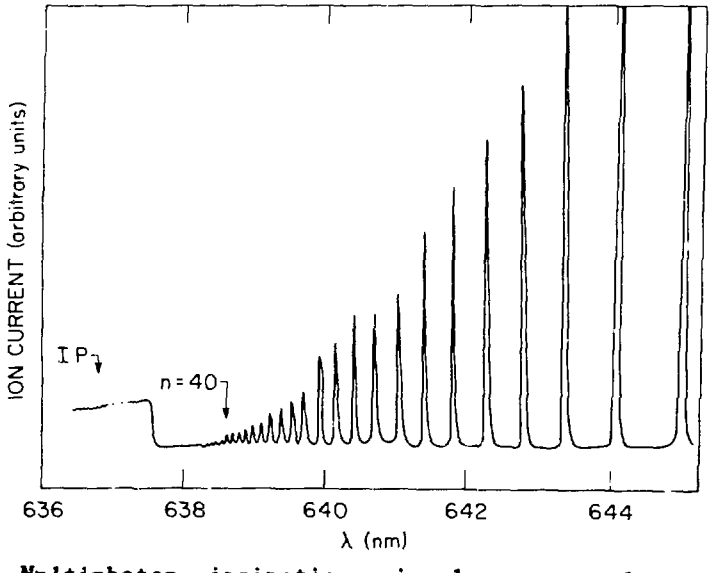

Fig. 8. Multiphoton ionization signal near the two-photon ionization threshold at 636.8 nm. The sharp peak represent two-photon resonant (nd level) three-photon ionization. The two-photon ionization "step" is observed below the zero field value at 636.8 due to field ionization.

For very low ion draw-out fields (<10 v/cm), weak signals are observed at the laser wavelength corresponding to two-photon excitation, three-photon ionization via the two-photon allowed ns levels. A component of the ns signal is seen to increase as the square of the electric field. We find for R[ns/(n-1)d], the ratio of MPI strength via an ns state to that via the (n-1) d5/2 state:

$$R[ns/(n-1)d_{5/2}] = \gamma_0 + \gamma\ (ns)\ |\vec{F}|^2 \qquad (4)$$

where γ_0 is less than 0.01 and where the coefficient γ is a strongly increasing function of n. We interpret this as follows: two-photon excitation oscillator strengths for ns and nd series are comparable. The cross section for subsequent photoionization of an ns state is expected to be quite small. For example, Pindzola (private communication) calculates the photoionization cross section for the 8s state to be ~4 x 10^{-4} times smaller than the 8d3/2 state and the 12s state to be 8 x 10^{-3} times smaller than the 12d3/2 state. An electric field mixes in the nearby np levels and it is this component of the Stark mixed state which is more readily photoionized. Figure 9 shows the field-induced signal at the 16s energy level. The effective quantum number is 12 (quantum defect = 4) and therefore 9 other higher angular momentum states are seen (one is hidden under the 16s signal). The remaining 12d and 12p states are not shown.

Field-induced MPI is also readily distinguished from a field-free component via its dependence on the angle between $\vec{E}$ and $\vec{F}$. We find

$$\gamma(ns) \sim 1 + 0.8 \cos^2\theta \quad . \qquad (5)$$

Increasing the electric field also permits normally forbidden MPI via the np series, but for a complementary reason. The field mixes a p state with a nearby s or d level, permitting two-photon access to the p series. Photoionization of the original p component then ensues. We show a typical field-induced np level in Fig. 10 for n = 13. The ratio of the p levels to the adjacent d levels follows:

$$R(nP_J/(n-1)d_{5/2}) = \gamma(np_J)\ |\vec{F}|^2 \qquad (6)$$

consistent with the proposed mechanism. The coefficient $\gamma(np_{3/2})$ is a rapidly increasing function of principal quantum number.[21] It is also a function of θ as shown in Fig. 11. We find

$$\gamma(np) \sim 1 + 0.55 \cos^2\theta + 2.66(\sin\theta \cos\theta)^2 \qquad (7)$$

and, for the ratio of spin-orbit components, $\gamma(np_{3/2})/\gamma(np_{1/2}) \simeq 4.5$ (± 0.5). This ratio, while not statistical is closer to the value 2 than the anomolously high values observed in one-photon absorption oscillator strengths.[22]

The relations reported here were obtained at sufficiently low electric fields that perturbation theory should still be valid. At higher fields we observe large-scale level shifts and the emergence

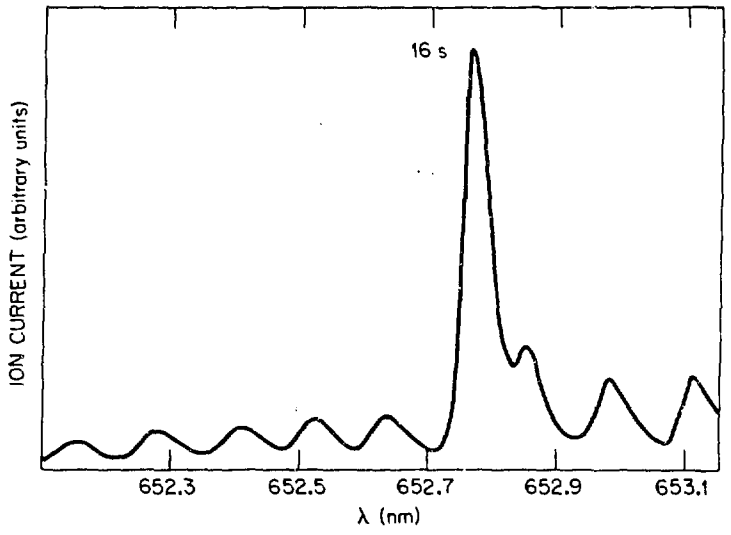

Fig. 9. Electric field enhanced three-photon ionization of $n\ell$ states of cesium near the 16s level. Field strength 3500 V/cm.

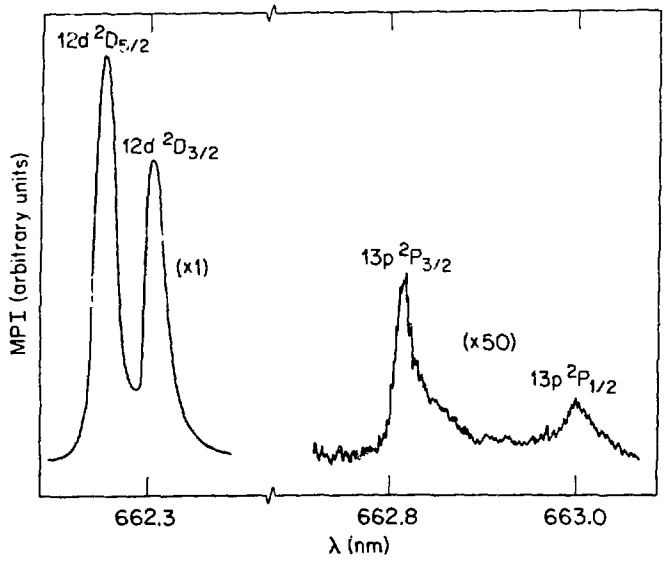

Fig. 10. Electric field induced three-photon ionization of atomic cesium in which the second photon is in resonance with the $13p^2P_{3/2,1/2}$ states. Electric field strength was 700 V/cm.

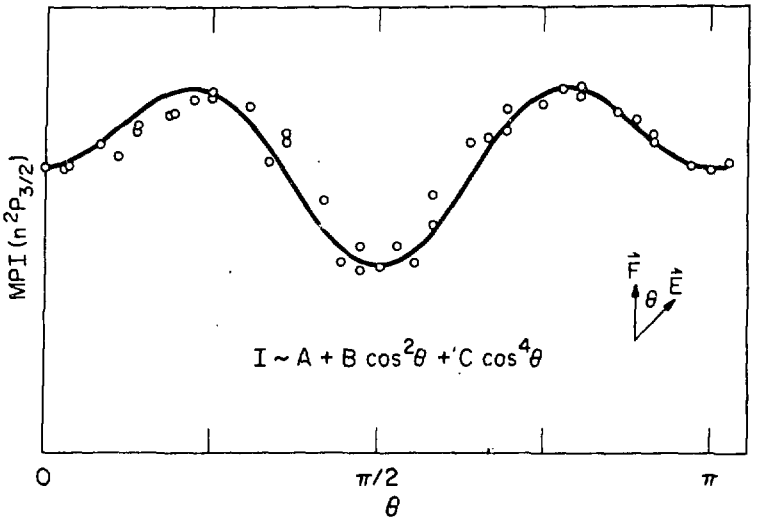

Fig. 11. Dependence of the field induced multiphoton ionization signal due to the $np^2P_{3/2}$ state (see Fig. 9) as a function of the angle between the laser polarization E and the electric field $\vec{F}$.

of complete Stark manifolds. Above the field-ionization limit we observe much fine structure, including some which persists to above the zero-field limit. Thus, a panoply of phenomena, already known in one-photon spectroscopy, can be studied, often to good advantage, via MPI.

CONCLUSIONS

We have presented new experimental results on two- and three-photon ionization photoelectron angular distributions for an alkali atom. The results clearly illustrate the importance of hyperfine mixing at the resonant intermediate level. Section B presents the first experimental studies of the effects of static electric fields upon MPI. The DC Stark effect is seen to induce ionization signals from electronic states which are normally absent due to symmetry selection rules or low photoionization cross sections. Much further experimental and especially theoretical work needs to be performed on Stark effects on MPI.

REFERENCES

[1] M. M. Lambropoulos and R. S. Berry, Phys. Rev. 8, 844 (1973).

[2] For reviews of various aspects of multiphoton ionization and photoelectron angular distribution see: P. Lambropoulos in ADVANCES IN ATOMIC AND MOLECULAR PHYSICS 12, 87-164 (Academic Press, New York, 1976); MULTIPHOTON PROCESSES (J. H. Eberly and P. Lambropoulos, Eds., Wiley, New York, 1978); and J. Morellec, D. Normands, G. Petite in ADVANCES IN ATOMIC AND MOLECULAR PHYSICS 18, 97-164 (Academic Press, New York, 1982).

[3] J. C. Tully, R. S. Berry, and R. J. Dalton, Phys. Rev. 176, 95 (1968).

[4] S. N. Dixit and P. Lambropoulos, Phys. Rev. Lett. 46, 1278 (1981).

[5] S. N. Dixit and P. Lambropoulos, Phys. Rev. A 27, 168 (1983).

[6] J. A. Duncanson, Jr., M. P. Strand, A. Lindgrard, and R. S. Berry, Phys. Rev. Lett. 37, 987 (1976).

[7] J. C. Hansen, J. A. Duncanson, Jr., R.-L. Chien, and R. S. Berry, Phys. Rev. A 21, 222 (1980).

[8] S. Edelstein, M. M. Lambropoulos, and R. S. Berry, Phys. Rev. A 9, 2459 (1974).

[9] H. Kaminski, J. Kessler, and K. J. Kollath, Phys. Rev. Lett. 45, 1161 (1980).

[10] D. Feldmann and K. H. Welge, J. Phys. B 15, 1651 (1982).

[11] G. Leuchs and S. J. Smith, J. Phys. B 15, 1051 (1982).

[12] M. P. Strand, J. Hansen, R.-L. Chien, and R. S. Berry, Chem. Phys. Lett. 59, 205 (1978).

[13] G. Leuchs, S. J. Smith, E. Khawaja, and H. Walther, Optic Comm. 31, 313 (1979).

[14] F. Fabre, P. Agostini, G. Petite, and M. Clement, J. Phys. B 14, L677 (1981).

[15] W. Ohmesorge, F. Diedrich, G. Leuchs, D. S. Elliott, H. Walther, Phys. Rev. 29, 1181 (1984).

[16] P. Agostini, F. Fabre, G. Mainfray, G. Petite, and N. K. Rahman, Phys. Rev. Lett. 42, 1127 (1979).

[17] See Richard R. Freeman, International Conference on Atomic Physics, 1980, in ATOMIC PHYSICS 7 (D. Kleppner and F. M. Pipkin, Eds.), Plenum Press, 1980.

[18] H. Kaminski, J. Kessler, and K. J. Kollath, Phys. Rev. Lett. 45, 1161 (1980).

[19] R. N. Compton, J.A.D. Stockdale, C. D. Cooper, X. Tang, and P. Lambropoulos, Phys. Rev. A (submitted).

[20] S. N. Dixit and P. Lambropoulos, Phys. Rev. A 27, 168 (1983).

[21] W. E. Cooke and T. F. Gallagher, Phys. Rev. A 17, 1226 (1978).

[22] E. Fermi, Z. Physik 59, 680 (1929).